Massively parallel photosensitive hydrogel encapsulated single-cell to a cluster of cells patterning and bone regeneration application

Sarin Abraham,[a] Gayathri R,[b] Kavitha Govarthanan,[a] Suresh Rao,[a] Moeto Nagai,[c] Tuhin Subhra Santra [a*]

[a] Department of Engineering Design, Indian Institute of Technology- Madras, India
[b]Department of Mechanical Engineering, Indian Institute of Technology-Madras, India
[c] Department of Mechanical Engineering, Toyohashi University of Technology, Aichi, Japan
Corresponding author email: tuhin@zmail.iitm.ac.in, santra.tuhin@gmail.com

Supplementary information

Table of contents

Table 1. A detailed comparison between our proposed work and other related works, including 3D printing, microfluidics, photolithography, stereolithography, and projection stereolithography
Procedure for scanning electron microscopy (SEM) imaging
Protocol for micro-pattern structure mineralization using Alizarin red staining
S1. Micro-patterns of size 60 µm x 60µm and an interspacing of 100 µm.
S2. Circular patterning of micro-patterns
S3. Effect of UV exposure time on U-87 MG cells in 5%(w/v) GelMA
S4. Effect of UV exposure time on U-87 MG cells in 10%(w/v) GelMA
S5. Effect of UV exposure time on U-87 MG cells in 15%(w/v) GelMA
S6. Effect of UV exposure on different GelMA concentrations for cell patterning
Effect of UV exposure intensity on cell viability
S7. Effect of UV intensity on U-87 MG cells in 5%(w/v) GelMA
S8. Effect of UV intensity on U-87 MG cells in 10%(w/v) GelMA
S9. Effect of UV intensity on U-87 MG cells in 15%(w/v) GelMA
S10. Growth of U-87 MG cells in 15%(w/v) GelMA, 10%(w/v) GelMA and 5%(w/v) GelMA
S11. Shape fidelity and edge sharpness analysis of GelMA micro-patterns
S12. ^{1}H NMR spectra of gelatin
S13. ^{1}H NMR spectra of GelMA
S14. U-87 MG cell line patterning using an array of 250µm x 250µm pattern size
S15. L929 cell line patterning using an array of 250µm x 250µm pattern size
S16. A431 cell line patterning using an array of 250µm x 250µm pattern size
S17. U-87 MG cell line patterning in 125µm x 125µm and 80µm x 80µm square micro-patterns
S18. Plot of patterning efficiency, cell viability and probability of single to cluster of cells
S19. XRD spectra of nano-hydroxyapatite powder

Patterning methodology	Microstructure pattern area	Exposure intensity (mW/cm^{-2})	Exposure time (seconds)	Patterning efficiency	Cell viability	Applications	Reference
3D Printing	10mm x 10mm square	6.9	30 , 60	Nil	85.7% ± 4.1%, 84.4% ± 0.4%	stiff tissue-engineered construct	[1]
Photolithography	400µm (loop diameter) x 150 µm (diameter) x 150 µm (h)	2.95	20	46.4 ± 7.8% - single cell, 55.2 ± 5.40% - cluster of cells	Good viability	Monitor the growth of single neurons and autapse formation	[2]
	50 µm to 200 µm sized micro-constructs	6.9	20	Nil	Nil	functional tissues - aligned cells	[3]
Stereolithographic 3D printing	Layer thickness ~900µm-diameter 8mm	Nil	30	Nil	cell (~ <5%) was found dead	tissue-engineered cartilage	[4]
Projection stereolithography	vascular networks 1.5 mm	7 to 16	15, 25, 35, and 45	Nil	75%,	3D vascular constructs	[5]
Photopatterning	mold (8 mm in diameter and 1 mm in depth)	3.5	5 minutes	93.7 ± 5.2% for cluster of cells	above 87%	Spheroid	[6]
Microfluidic technology	channel has a width of 600 µm	25	40	Nil	over 90 %	Dentin on chip	[7]
Our proposed work	80 µm x 80 µm to 250 µm x 250 µm micropattern size	2.4	12 to 18	~54.23% probability for encapsulating single cell ~ 100% patterning efficiency for cluster of cells ~13 cells	~ 97.21%	replicate complex tissue engineering patterns and bone tissue regeneration	

Table 1: A detailed comparison between our proposed work and other related works, including 3D printing, microfluidics, photolithography, stereolithography, and projection stereolithography

Procedure for scanning electron microscopy (SEM) imaging

Firstly, a polydimethylsiloxane (PDMS) well of 10 mm in height and a diameter of 3 cm is fabricated by combining a curing agent in a 10:1 ratio (Silicone elastomer kit, SYLGARD). GelMA solutions for different concentrations were prepared, and poured into the above PDMS wells attached to a glass substrate, and later photopolymerized by exposing the solution to UV light for 3 minutes. The polymerized GelMA samples were immersed in 1 x PBS overnight. Later, the samples were lyophilized for 2 days and the SEM images were captured.[8]

Protocol for micro-pattern structure mineralization using Alizarin red staining

Initially, cell culture media was removed from the patterned samples and the samples were rinsed with PBS two times. Then, the samples were fixed by 20 minutes incubation in 2% paraformaldehyde, followed by washing in PBS. Later, 40mM alizarin red solution was introduced on the micropatterned device and incubated at room temperature for 20 min. After that, the device was rinsed using PBS thrice to remove any excess dye and imaged under a microscope (IX 73, Olympus, Japan). For quantitative analysis, samples were treated with 10%(v/v) acetic acid for 30 min at 25°C under mild shaking. Finally, dissolved dyes were

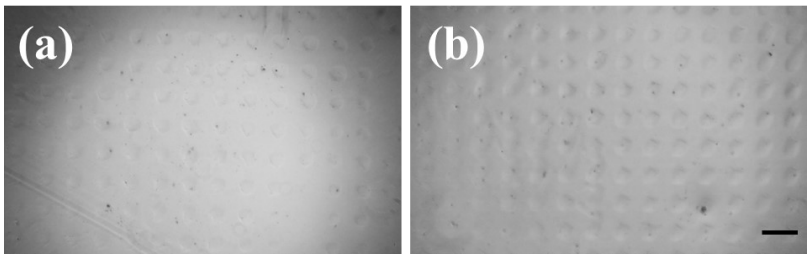

Figure S1: Micro-patterns on TMSPMA treated glass slides of size 60µm x 60µm and an interspacing of 100 µm. Figures (a - c) shows the brightfield images for 10%(w/v) GelMA when exposed to 2.4mW/cm^2 UV intensities for 19 seconds. With these set parameters, we were unable to obtain good patterns and cell encapsulation was also not achieved. Scale for images is 300µm.

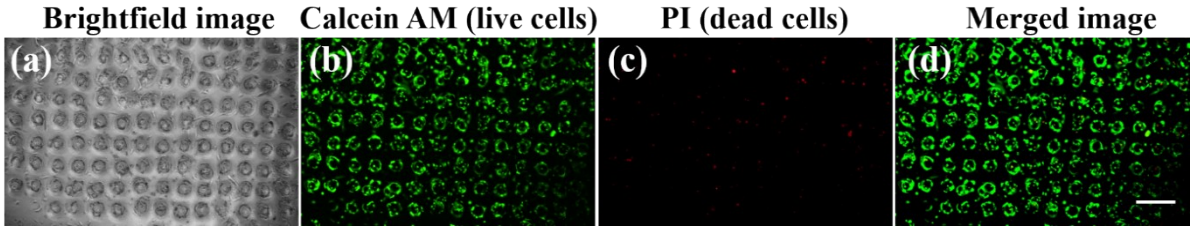

Figure S2: Circular patterns on TMSPMA treated glass slides. Figure (a) shows the brightfield images for 10%(w/v) GelMA when exposed to 2.4mW/cm^2 UV intensities. Figure (b) indicates the live cells and Figure (c) shows the dead cells, and the merged image indicating the live and dead cells is shown in Figure (d) for a circular pattern of diameter 100µm. Scale for images is 300µm.

transferred into a 96-well plate and its absorbance reading was performed at 405 nm wavelength using BioTek multimode plate reader and then analyzed using Gen6 sofware.[9]

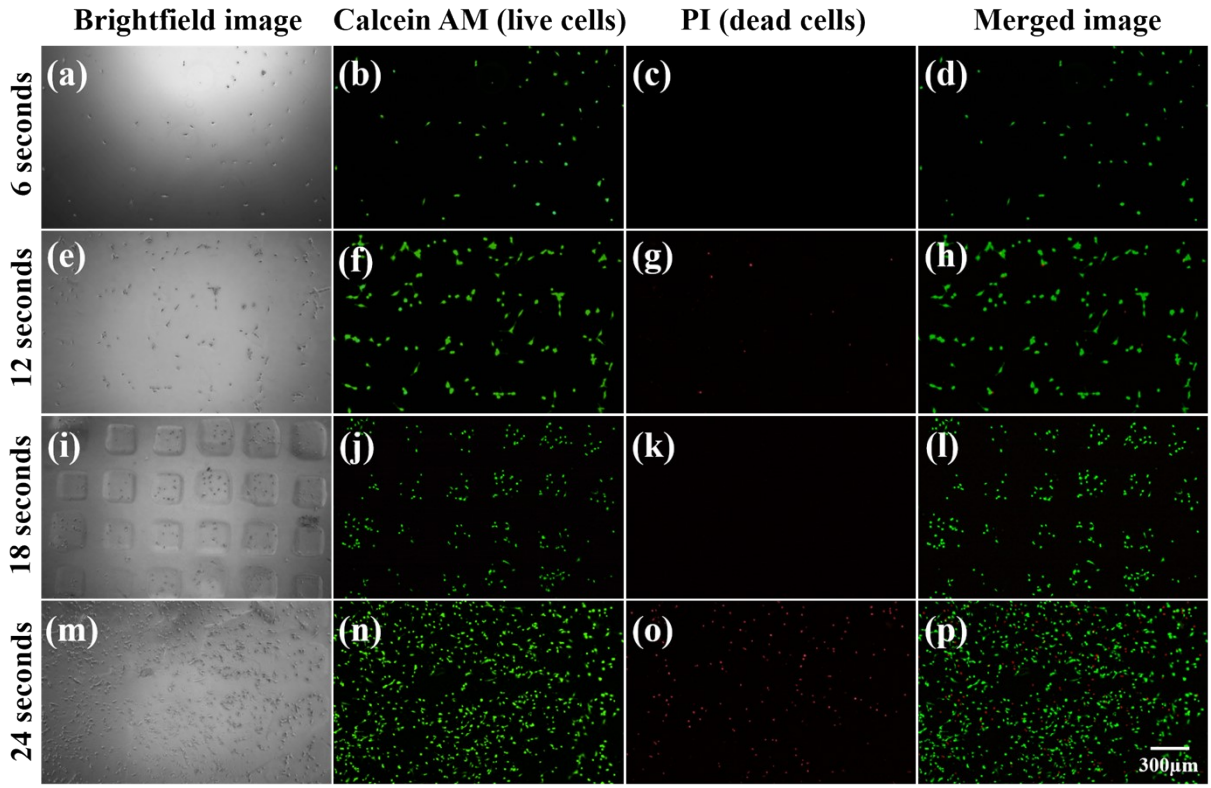

Figure S3: Effect of UV exposure time on U-87 MG cells in 5%(w/v) GelMA for 250µm x 250µm micro-pattern array. Figure (a -d) shows the brightfield image, live cells, dead cells and merged image for 5%(w/v) GelMA when exposed to a UV exposure time of 6 seconds. Similarly, Figure (e- h) indicates results for 12 seconds exposure, Figure (i- l) shows the corresponding results for 18 seconds of exposure time and Figure (m – p) shows the results for 24 seconds exposure.

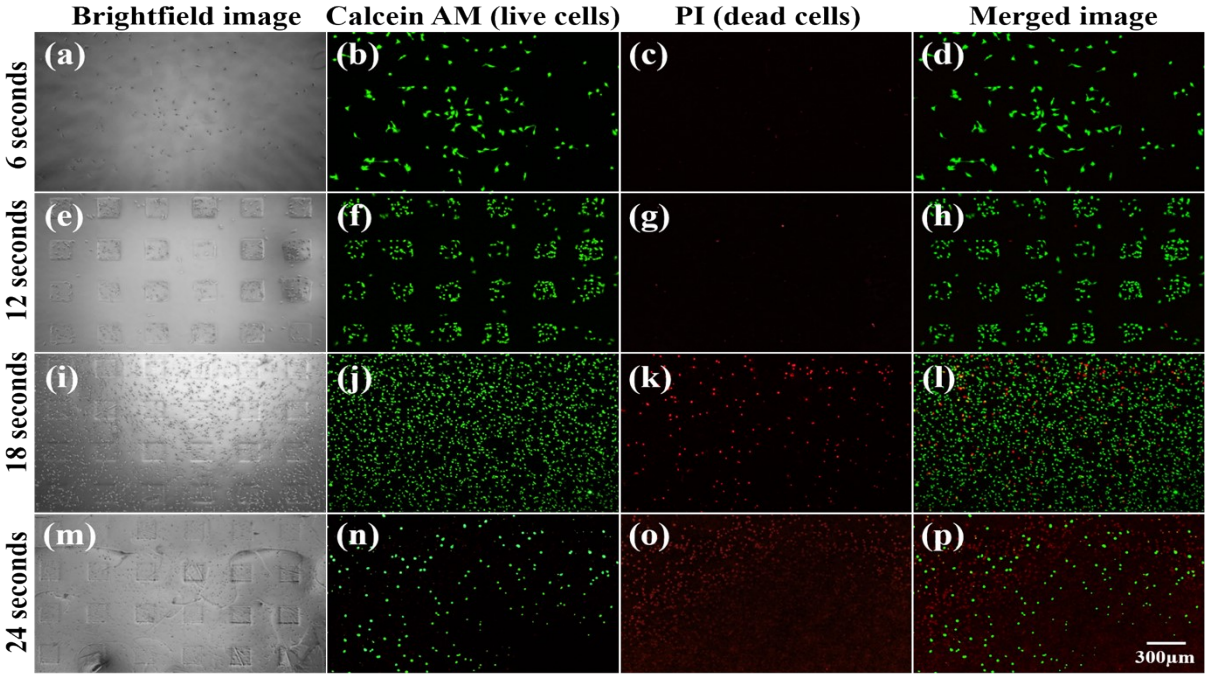

Figure S4: Effect of UV exposure time on U-87 MG cells in 10%(w/v) GelMA for 250µm x 250µm micro-pattern array. Figure (a -d) shows the brightfield image, live cells, dead cells and merged image for 10%(w/v) GelMA when exposed to a UV exposure time of 6 seconds. Similarly, Figure (e- h) indicates results for 12 seconds exposure, Figure (i- l) shows the corresponding results for 18 seconds of exposure time and Figure (m – p) shows the results for 24 seconds exposure.

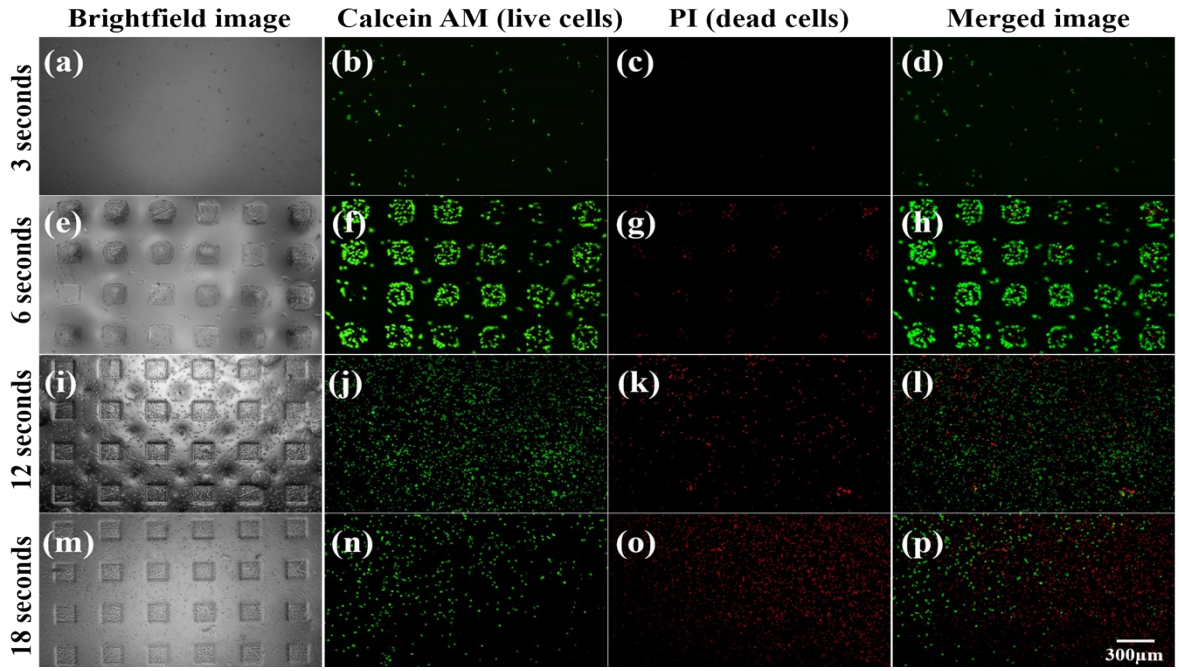

Figure S5: Effect of UV exposure time on U-87 MG cells in 15%(w/v) GelMA for 250µm x 250µm micro-pattern array. Figure (a -d) shows the brightfield image, live cells, dead cells and merged image for 15%(w/v) GelMA when exposed to a UV exposure time of 3 seconds. Similarly, Figure (e- h) indicates results for 6 seconds exposure, Figure (i- l) shows the corresponding results for 12 seconds of exposure time and Figure (m – p) shows the results for 18 seconds exposure.

Effect of UV exposure intensity on cell viability

Experiments were conducted as we optimized exposure intensity of the UV source for 250µm x 250µm micro-pattern array using U-87 MG cells. We started with the lowest intensity of 2.4mW/cm^2 and exposed 5%(w/v) GelMA for 18 seconds, and good patterns with a high cell viability of approximately 97.16 % was obtained. However slight distortion in the pattern was observed after 10 hours of patterning which may be attributed to the high swelling ration of 5%(w/v) GelMA.[10] When the intensity was further increased to 4.5 mW/cm^2 and 9 mW/cm^2 while maintaining the same exposure time of 18 seconds, the cell viability reduced to 77.9%

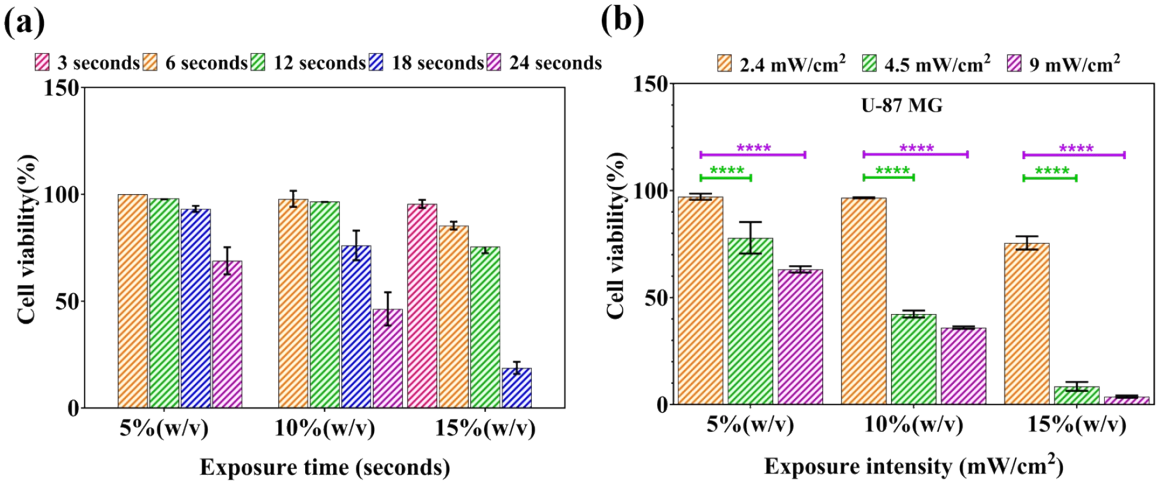

Figure S6: Effect of UV exposure on different GelMA concentrations for cell patterning (a) Cell viability with different exposure time for 5%(w/v), 10%(w/v) and 15%(w/v) GelMA (b) Cell viability with different UV intensity for 5%(w/v), 10%(w/v) and 15%(w/v) GelMA. Data are presented as the mean and SD of the three independent experiments. Statistical analysis was performed using two-way ANOVA test.

and 63.17%, respectively but the patterns were overexposed. The live-dead staining images captured after 10 hours of patterning are depicted in Figure S7.

A similar experiment was carried out for 10%(w/v) GelMA. When the sample was exposed to 2.4mW/cm^2 for 12 seconds the cell viability was the highest with 96.64%. As the intensity was further increased to 4.5 mW/cm^2 and 9 mW/cm^2 with the exposure time held constant at 12

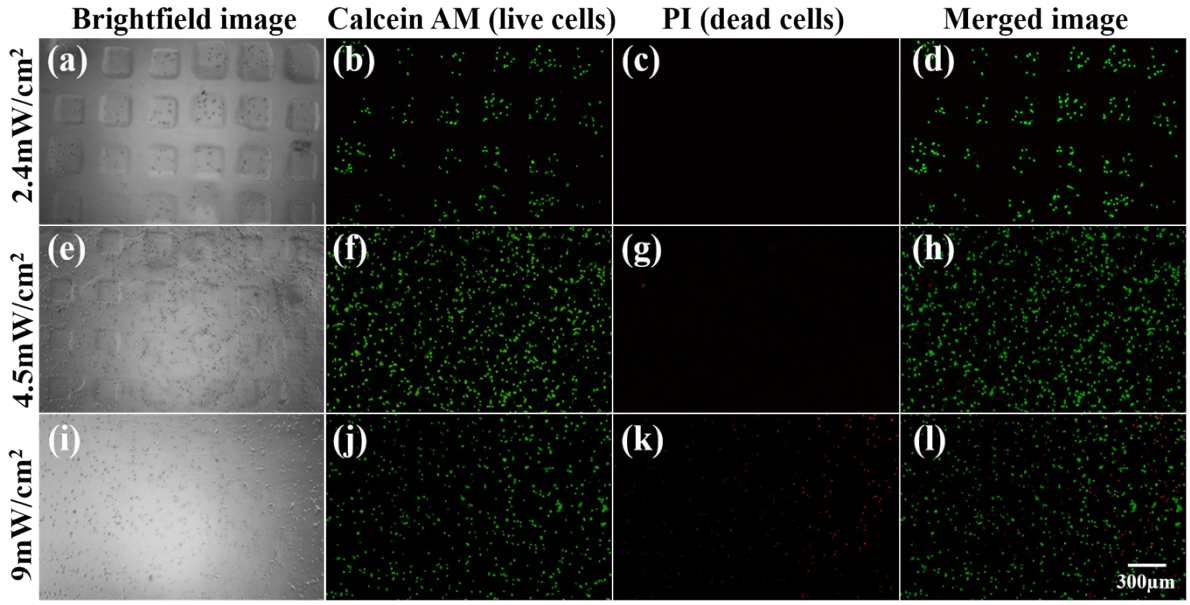

Figure S7: Effect of UV intensity on U-87 MG cells in 5%(w/v) GelMA for 250µm x 250µm micro-pattern array. Figure (a -d) shows the brightfield image, live cells, dead cells and merged image for 5%(w/v) GelMA when exposed to an UV intensity of 2.4mW/cm^2 for 18 seconds. Similarly, Figure (e- h) indicates results for 4.5mW/cm^2 UV intensity and Figure (i- l) shows the corresponding results for 9mW/cm^2 of UV intensity.

seconds, cell viability decreased to 42.3% and 35.97%, respectively, resulting in overexposed patterns. The effect of UV intensity on the U-87 MG cell line is depicted in Figure S8.

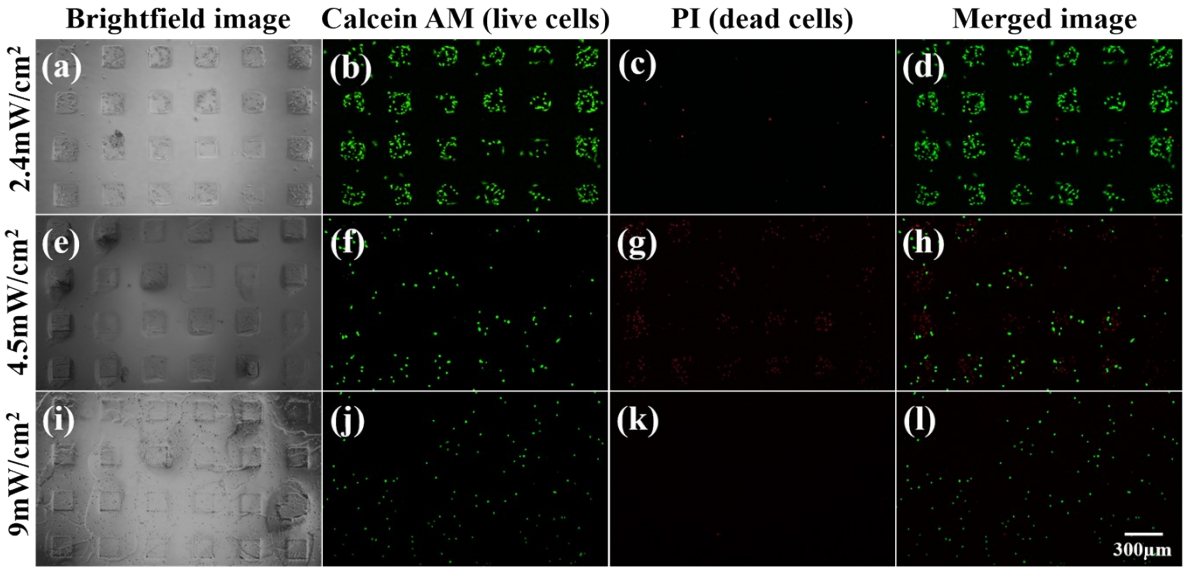

Figure S8: Effect of UV intensity on U-87 MG cells in 10%(w/v) GelMA for 250µm x 250µm micro-pattern array. Figure (a -d) shows the brightfield image, live cells, dead cells and merged image for 10%(w/v) GelMA when exposed to an UV intensity of 2.4mW/cm^2 for 12 seconds. Similarly, Figure (e- h) indicates results for 4.5mW/cm^2 UV intensity and Figure (i- l) shows the corresponding results for 9mW/cm^2 of UV intensity.

Subsequently, an experiment was conducted for 15%(w/v) GelMA. When the sample was exposed to 2.4mW/ cm^2 for 6 seconds, and cell viability of 75.52% was achieved. As the intensity was increased to 4.5 mW/cm^2 and 9 mW/cm^2, the cell viability reduced to 8.5% and 3.70% respectively. The effect of UV intensity on the U-87 MG cell line is depicted in Figure S9. The cell viability in percentage for the three GelMA concentrations for varying UV intensity is shown in Figure S6(b). With the optimizations established, we determined the optimal balance of UV intensity and exposure time needed for effective polymerization without compromising cell viability or pattern quality across all three GelMA concentrations. Consequently, the UV intensity was set to 2.4 mW/cm^2 for the subsequent experiments, which resulted in higher cell viability and improved patterning efficiency. The exposure times were 18 seconds for 5% (w/v) GelMA, 12 seconds for 10% (w/v) GelMA, and 6 seconds for 15% (w/v) GelMA.

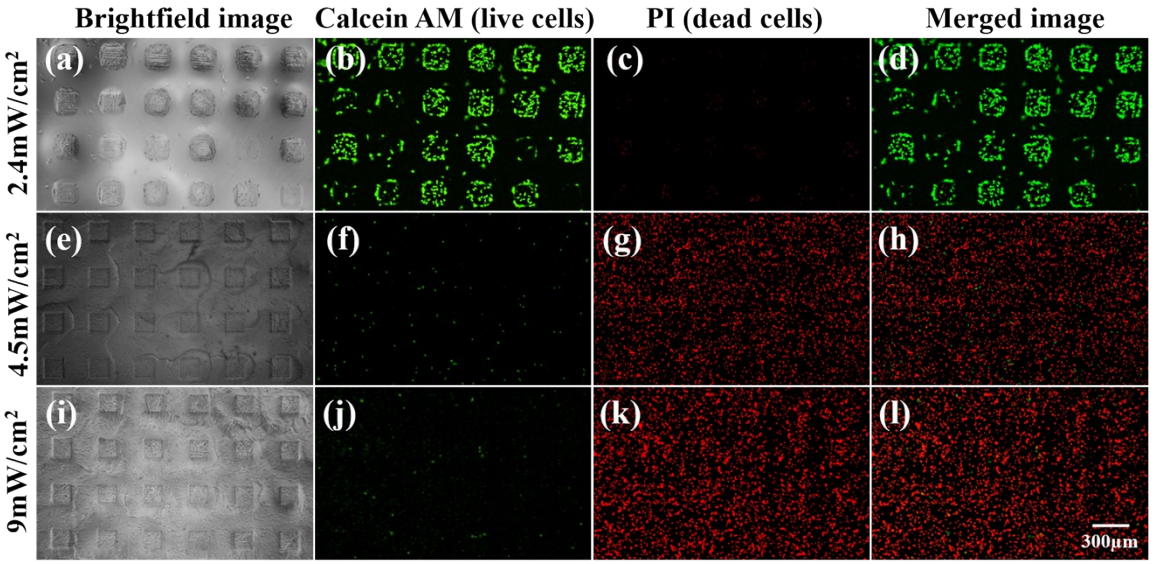

Figure S9: Effect of UV intensity on U-87 MG cells in 15%(w/v) GelMA for 250µm x 250µm micro-pattern array. Figure (a -d) shows the brightfield image, live cells, dead cells and merged image for 15%(w/v) GelMA when exposed to an UV intensity of 2.4mW/cm^2 for 6 seconds. Similarly, Figure (e- h) indicates results for 4.5mW/cm^2 UV intensity and Figure (i- l) shows the corresponding results for 9mW/cm^2 of UV intensity.

.

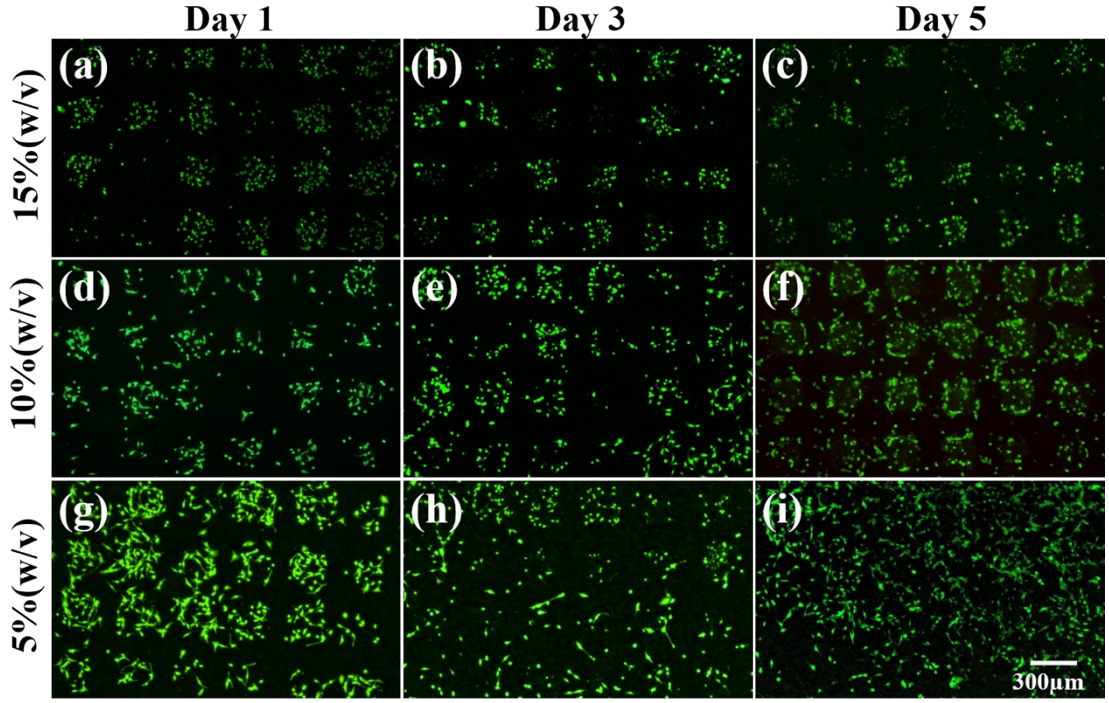

Figure S10: Cell growth of U-87 MG cells line in 15%(w/v) GelMA, 10%(w/v) GelMA and 5%(w/v) GelMA. Figure (a, d, g) shows the live cells on day 1 for 15%(w/v) GelMA, 10%(w/v) GelMA and 5%(w/v) GelMA. Figure (b, e, h) shows the live cells on third day and Figure (c, f, i) shows the live cells on day 5.

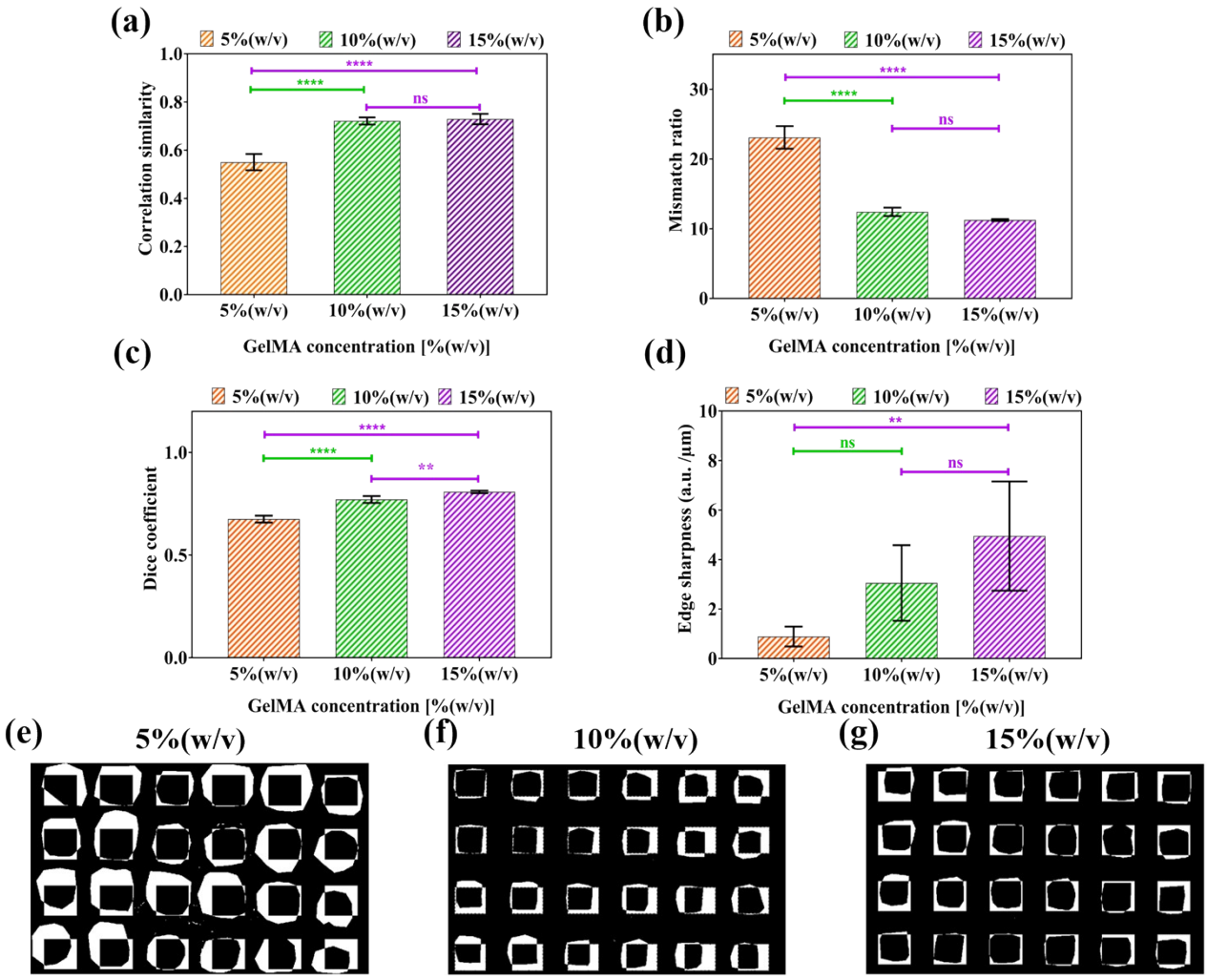

Figure S11: Shape fidelity analysis of GelMA micro-patterns across three concentrations (5%, 10%, and 15% w/v) (a) correlation similarity (b) the mismatch ratio (c) comparison of dice coefficient (d) comparison of edge sharpness (e -g) shows the mismatch map between the mask used for patterning and the patterned device fabricated using 5, 10 and 15%(w/v) GelMA concentrations. Statistical analysis was performed using one way ANOVA test with 3 unique trials per conditions.

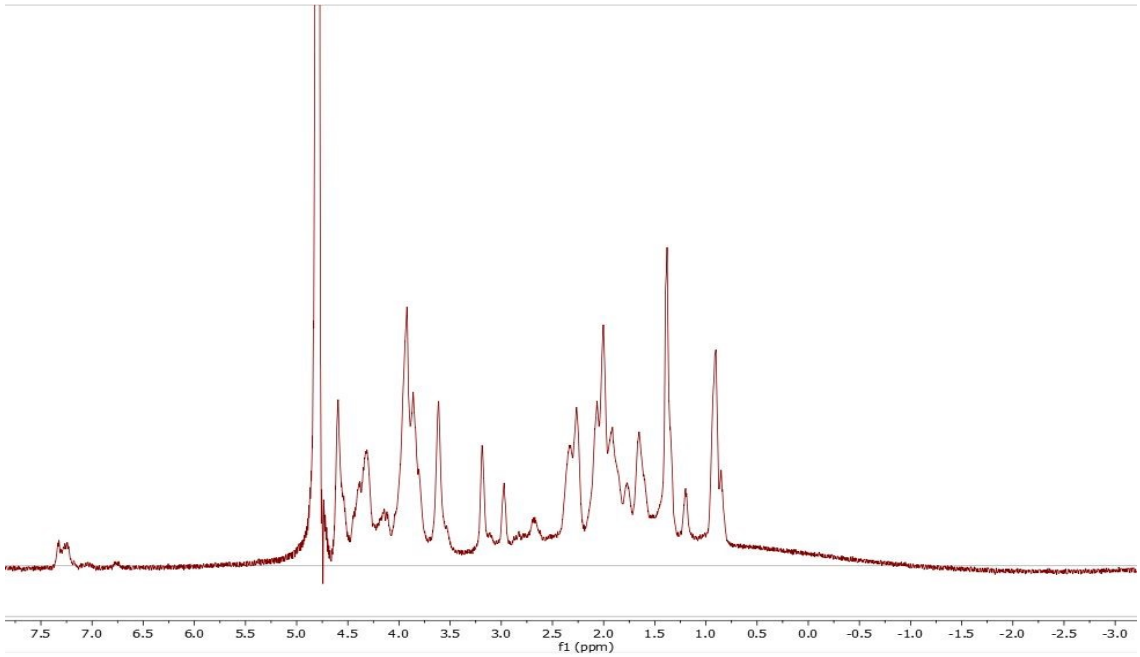

Figure S12: ^{1}H NMR spectra of gelatin

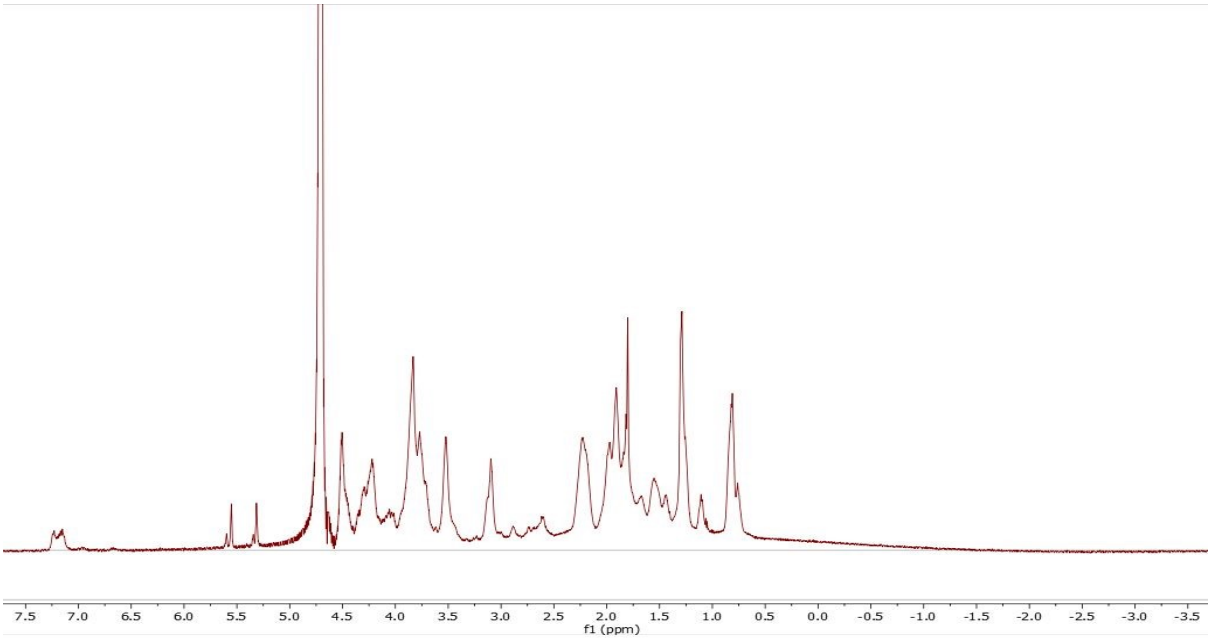

Figure S13: ^{1}H NMR spectra of GelMA

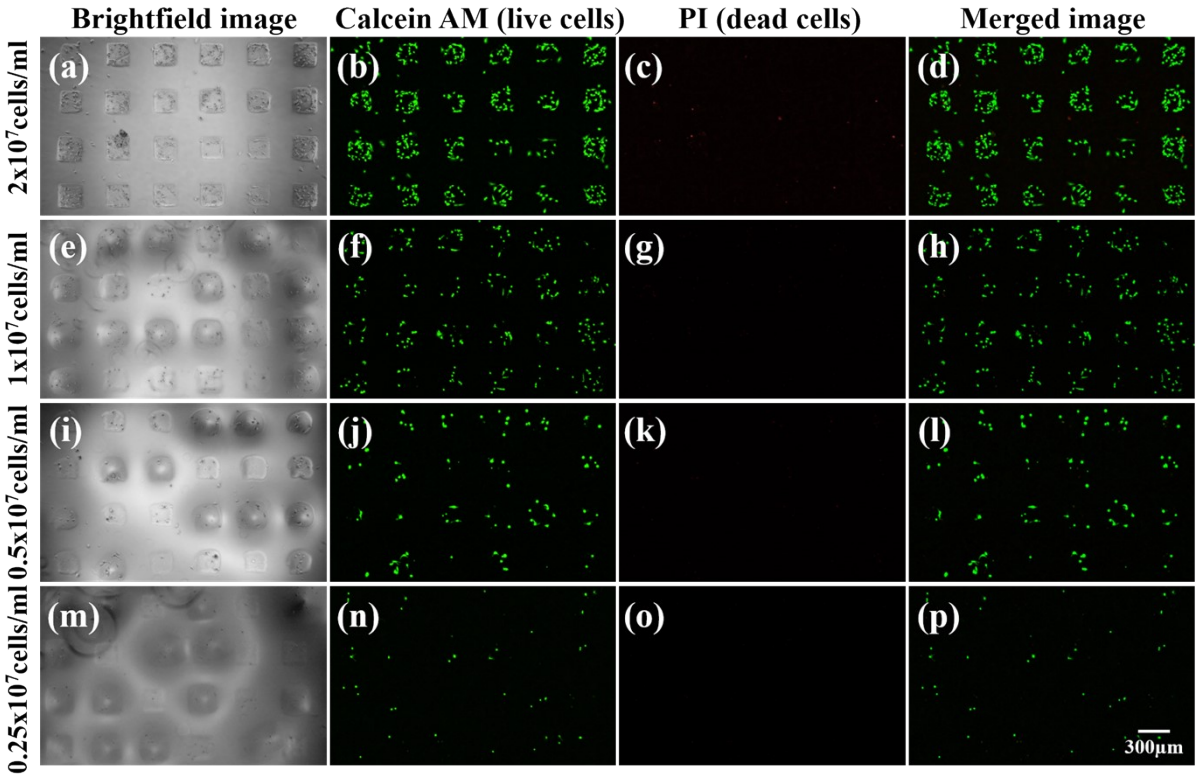

Figure S14: U-87 MG cell line patterning using an array of 250µm x 250µm pattern size and an interspacing of 200 µm. (a, e, i, m) indicate the brightfield images for different concentration of cells within the micro-pattern, (b, f, j, n) indicate the live cells stained using Calcein AM, (c, g, k, o) indicate the dead cells stained using PI dye and (d, h, l, p) shows merged image of the live and dead cells within the micro-pattern.

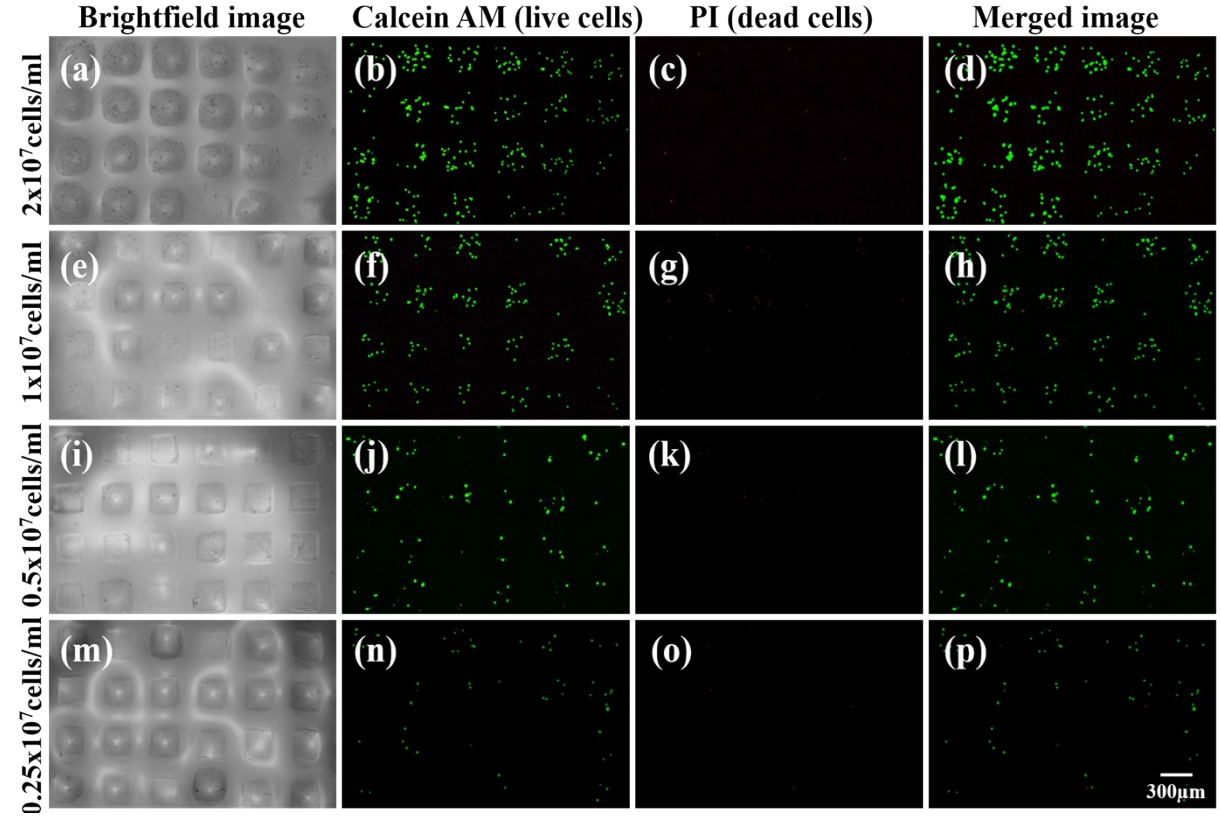

Figure S15: L929 cell line patterning using an array of 250µm x 250µm pattern size and an interspacing of 200 µm. (a, e, i, m) indicate the brightfield images for different concentration of cells within the micro-pattern, (b, f, j, n) indicate the live cells stained using Calcein AM, (c, g, k, o) indicate the dead cells stained using PI dye and (d, h, l, p) shows merged image of the live and dead cells within the micro-pattern.

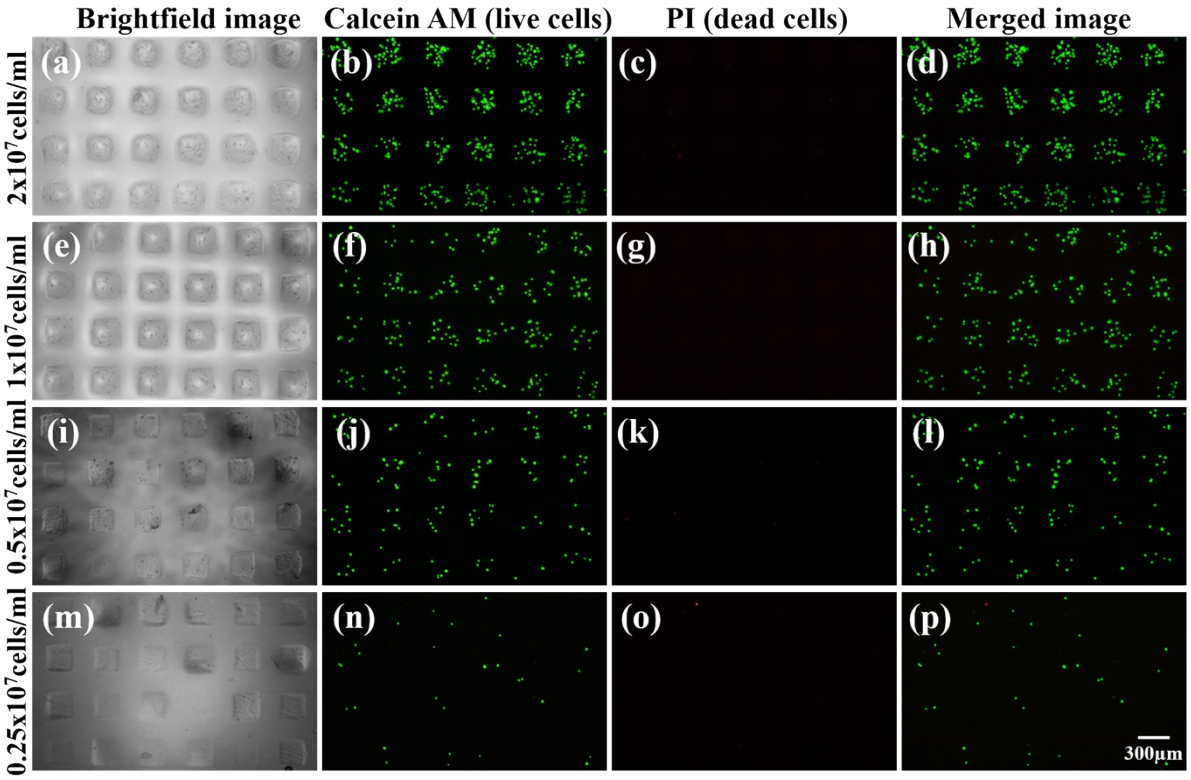

Figure S16: A431 cell line patterning using an array of 250µm x 250µm pattern size and an interspacing of 200µm. (a, e, i, m) indicate the brightfield images for different concentration of cells within the micro-pattern, (b, f, j, n) indicate the live cells stained using Calcein AM, (c, g, k, o) indicate the dead cells stained using PI dye and (d, h, l, p) shows merged image of the live and dead cells within the micro-pattern.

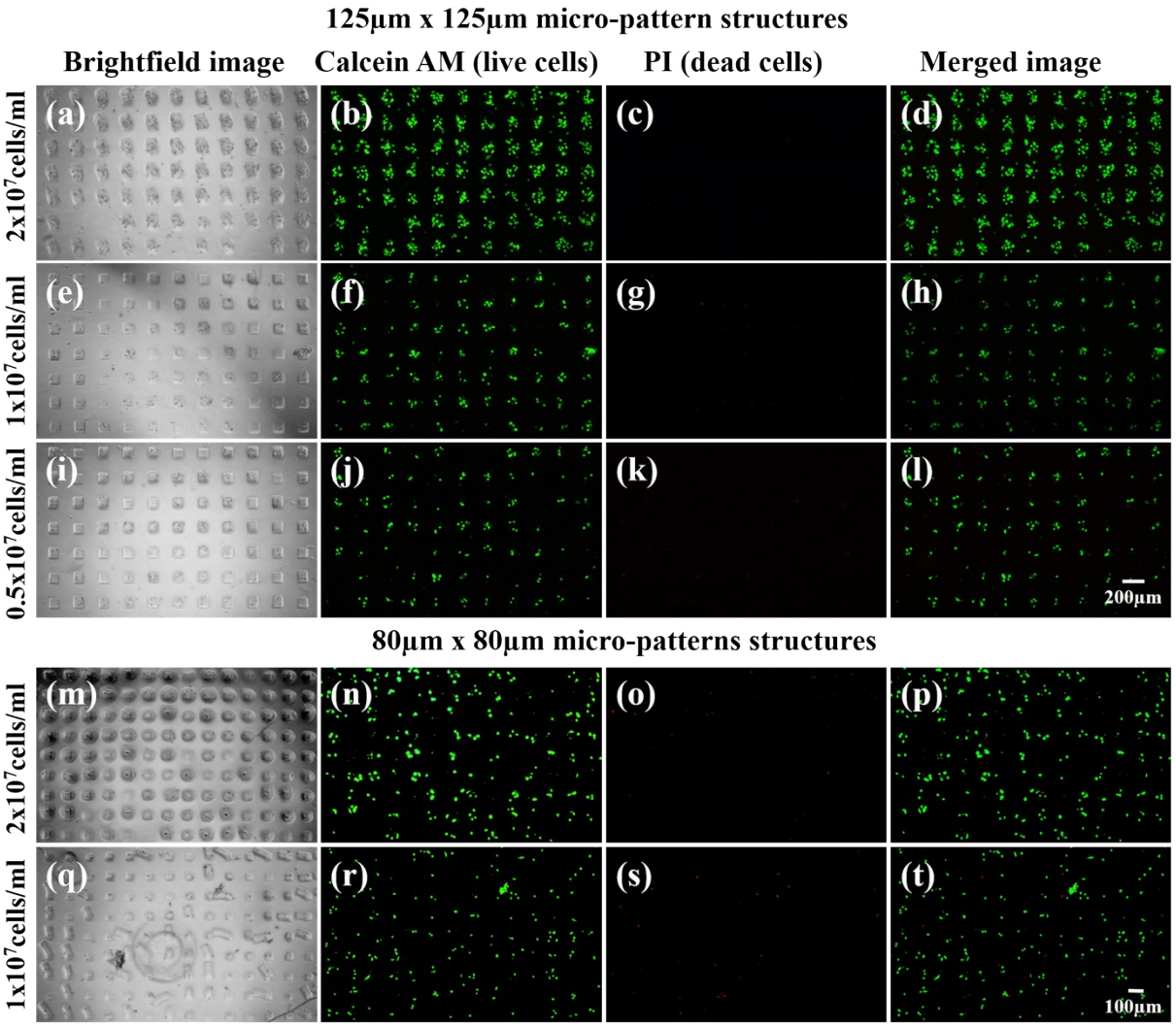

Figure S17: U-87 MG cell line patterning in 125µm x 125µm and 80µm x 80µm square micro-patterns. Figure (a, e, i) indicate the brightfield images for different concentration of cells for 125µm x 125µm micro-pattern array, (b, f, j) indicate the corresponding live cells stained using Calcein AM, (c, g, k) indicate the dead cells stained using PI dye for 125µm x 125µm array, (d, h, l) shows merge image of the live and dead cells within the micro constructs for 125 µm pattern size. Figure (m,n) indicated the indicate the brightfield images for different concentration of cells embedded in micro-pattern of size 80µm x 80µm , (n,r) indicate the live cells stained using Calcein AM, (o,s) indicate the dead cells stained using PI dye and (p,t) shows merge image of the live and dead cells within the micro constructs for 80µm pattern size.

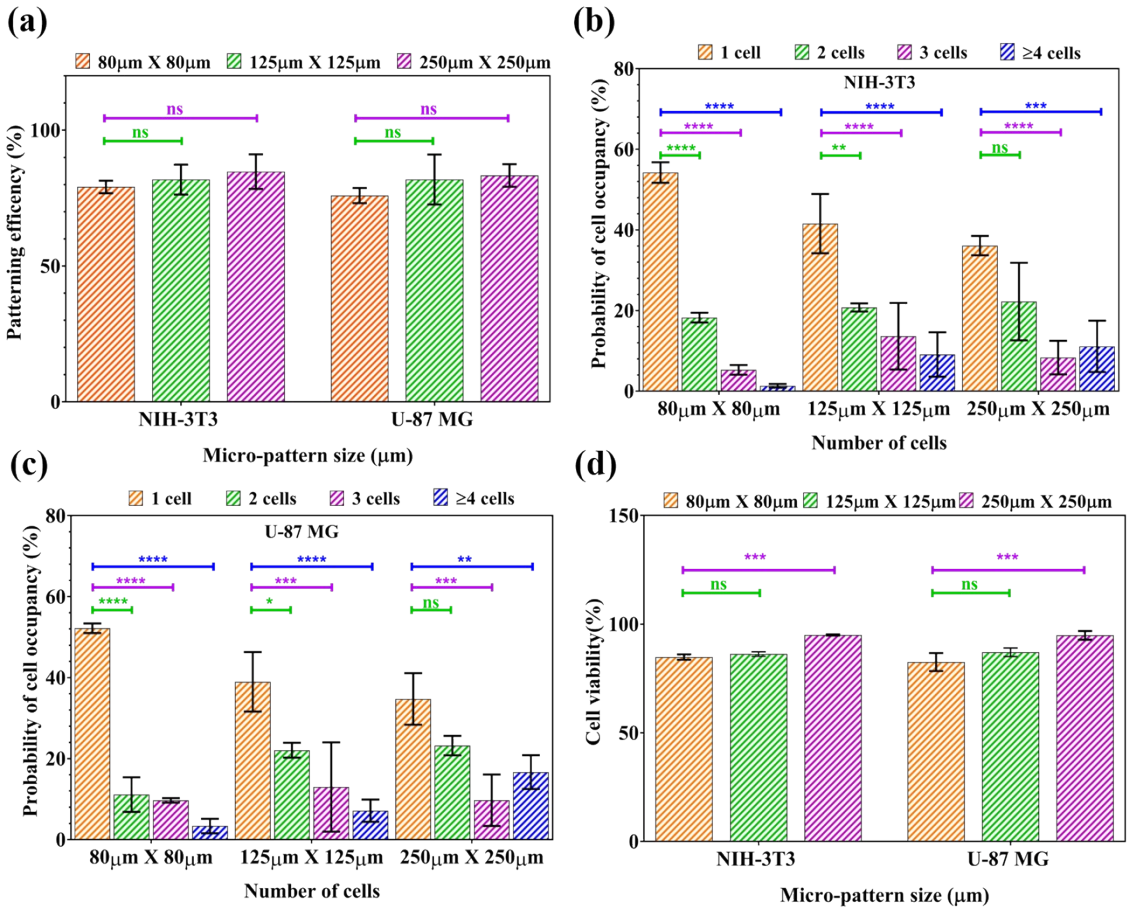

Figure S18: (a) Effciency for single to quartets patterning of NIH-3T3 cells for a concentation of 1 x 10^7 cells/mL for 80µm x 80µm micro-pattern size, 0.5 x 10^7 cells/mL for 125µm x 125µm micro-pattern size and 0.25x10^7 cells/mL for 250µm x 250µm micro-pattern size (b) effciency for single to quartets patterning of U-87 MG cells for concentation of 1 x 10^7 cells/mL for 80µm x 80µm micro-pattern size, 0.5 x 10^7 cells/mL for 125µm x 125µm micro-pattern size and 0.25x10^7 cells/mL for 250µm x 250µm micro-pattern size (c) probability of patterning single to quartets cells of NIH-3T3 for a concentation of 1 x 10^7 cells/mL for 80µm x 80µm micro-pattern size, 0.5 x 10^7 cells/mL for 125µm x 125µm micro-pattern size and 0.25x10^7 cells/mL for 250µm x 250µm micro-pattern size (d) probability of patterning single to quartets cells of U-87 MG cells for a concentation of 1 x 10^7 cells/mL for 80µm x 80µm micro-pattern size, 0.5 x 10^7 cells/mL for 125µm x 125µm micro-pattern size and 0.25x10^7 cells/mL for 250µm x 250µm micro-pattern size. Data are presented as the mean and SD of the three independent experiments. Statistical analysis was performed using two-way ANOVA test.

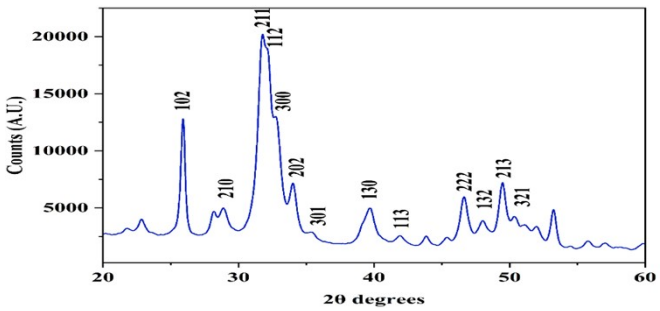

Figure S19: XRD spectra of nano-hydroxyapatite powder

References:

1 G. Basara, X. Yue and P. Zorlutuna, Gels, 2019, **3**.

2 Y. Fan, F. Xu, G. Huang, T. J. Lu and W. Xing, *Lab Chip*, 2012, **12**, 4724–4731.

3 Hug Aubin, J. W. Nichol, Ché B. Hutson, H. Bae, A. L. Sieminski, D. M. Cropek, P. Akhyari and A. Khademhosseini, *Biomaterials*, 2010, **31**, 6941–6951.

4 T. Lam, T. Dehne, J. P. Krüger, S. Hondke, M. Endres, A. Thomas, R. Lauster, M. Sittinger and L. Kloke, *J Biomed Mater Res B Appl Biomater*, 2019, **107**, 2649–2657.

5 S. Krishnamoorthy, S. Wadnap, B. Noorani, H. Xu and C. Xu, Eur Polym J, 2020, **124**.

6 M. Zhu, Y. Wang, G. Ferracci, J. Zheng, N. J. Cho and B. H. Lee, Sci Rep, 2019, **9**,6863.

7 H. Zhang, L. Li, S. Wang, X. Sun, C. Luo and B. Hou, *J Dent*, 2024, **146**, 105028.

8 J. W. Nichol, S. T. Koshy, H. Bae, C. M. Hwang, S. Yamanlar and A. Khademhosseini, *Biomaterials*, 2010, **31**, 5536–5544.

9 M. P. Bernardo, B. C. R. da Silva, A. E. I. Hamouda, M. A. S. de Toledo, C. Schalla, S. Rütten, R. Goetzke, L. H. C. Mattoso, M. Zenke and A. Sechi, *Sci Rep*, 2022, **12**, 1–15.

10 V. A. Liu and S. N. Bhatia, *Biomed Microdevices*, 2002, **4**, 257–266.